

Changes of daily precipitation extremes in the Himalayan range within China, 1978-2016

Jun Li*, Yuandi Zhao

School of Civil Engineering, Sichuan University of Science & Engineering, Zigong 643000, China

*Correspondence author: Lijunxiaoyouxiang@163.com

Keywords: Precipitation extremes, Temporal and spatial change, Himalayan range within China, South Asia Summer Monsoon

Abstract: The temporal and spatial changes of trends for extreme precipitation indices were analyzed on account of precipitation records at 9 meteorological stations in Himalayan range within China from 1978 to 2016. The results contain three parts. Firstly, the temporal and spatial changes of trends for precipitation extreme indices are irregular in Himalayan range with China. For regional pattern, only the consecutive dry days (CDD) has a statistically significant increasing trend of 3.17 days/decade over Himalayan range within China. Most of the other indices have statistically significant decreasing trends except CWD and SDII. The regionally averaged consecutive wet day (CWD) is stationary. The regionally averaged simple daily intensity index (SDII) is slightly increasing trend. For individual stations, many stationary trends are observed in heavy, very heavy and extremely heavy precipitation days (R10, R20 and R25). Most of the precipitations on very wet days (R95) have decreasing trends, but they are not statistically significant. Most of the precipitations on extremely wet days (R99) have stationary trends. Increasing and decreasing trends are observed in RX1day, RX5day, SDII and NW. The obvious trends of individual station are detected in PRCPTOT. Secondly, annual total precipitation and precipitation extremes indices have significant correlations based on the methods of Pearson's correlation and two-tailed t-test, except consecutive dry days (CDD). Thirdly, the South Asia Summer Monsoon evolution influence the trend changes of most precipitation extreme indices in the Himalayan range within China.

1. Introduction

The Himalayan ranges from the western syntaxis at its peaks of Nanga Parbat to southern that of peaks of Namche Barwa. The boundaries of Himalayan range are Yalu Tsangpo and Indus River from north and Main Frontal Thrust from South respectively (Ding et al., 2017; Yin, 2006; Zhang et al., 2016) (Fig. 1A). This region is about 2500 km in averaged length, 100 km in averaged width, with an area of $0.25 \times 10^6 \text{ km}^2$ and a population of 60 million approximately. In Himalayan range, numerous extreme precipitation events have been found. The types of extreme precipitation events include avalanches, glacial lake outburst floods (GLOFs), droughts, flash floods, landslides and debris flows. Such as a huge ice avalanche with a total volume of $0.7 \times 10^8 \text{ m}^3$ occurred at Aru village of Ali district on July 17th, 2016 (Tian et al., 2016), a GLOF with a peak discharge of $1.6 \times 10^4 \text{ m}^3$ occurred at Cirenmaco glacial lake on July 11th, 1981 (Chen et al., 2007; Delaney and Evans, 2015; Wang et al.,

2015), a super large landslide with a volume of $3 \times 10^8 \text{m}^3$ was occurred in Zhamunong gully on April 9th, 2000 (Delaney and Evans, 2015; Shang et al., 2003; Zhou et al., 2016). Many of those extreme precipitation events have had a negative impact upon the human safety and property in Himalayan range. In order to understand the characteristics, causes and mechanisms of extreme precipitation events, many studies relevant to changes in precipitation extremes have been conducted in the Himalayan range and adjacent area. Wang investigate recent changes in extremes of precipitation over the western Tibetan Plateau during 1973-2011, there are nonsignificant for the change of precipitation extremes (Wang et al., 2013). Sigdel compare the trends of precipitation extreme indices between the northern slopes and southern slopes in the central Himalaya, and conclude the consecutive dry days (CDD) and highest precipitation amount in 1-day period (RX1day) indices display similar increases on both the northern and southern slopes of the central Himalaya, but trends of other precipitation extreme indices are different (Sigdel and Ma, 2016). Zhang investigate the changes in frequency, intensity and monthly changes of precipitation extremes and discuss the impacts of the South Asian Summer Monsoon (SASM) on 12 precipitation indices in Southeastern Tibet (Zhang et al., 2015). More frequent precipitation extreme events will likely occur in Nepal based on the daily precipitation data from 1971 to 2006 (Baidya et al., 2008). It is found that 10 precipitation indices increase spatially from west to east over Mt. Qomolangma region (Lu et al., 2014). Based on the research of changes of precipitation extremes in Hengduan Mountains next to Himalayan range, consecutive dry days (CDD) and wet days precipitation are significant at the 5% level in the region (Ning et al., 2012), the regional trends generally decrease from the south to the north in Hengduan Mountains (Li et al., 2011; Zhang et al., 2014).

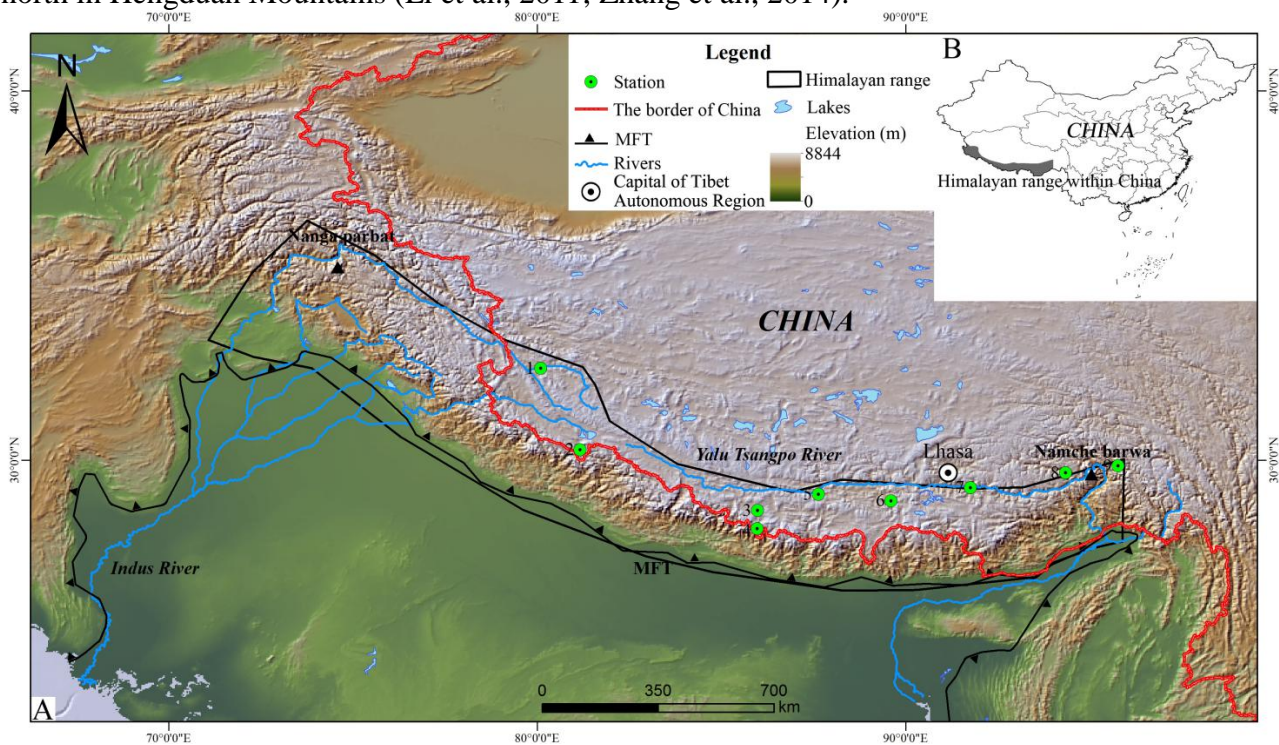


Figure 1: Meteorological station in the Himalayan range within China.

The names of meteorological stations correspond to the serial numbers in the Fig. 1. No.1-No.9 are the Shiquanhe station, Purang station, Tingri station, Nyalam station, Lhazê station, Gyangzê station, Tsedang station, Nyingchi station, Bome station in Table 1, respectively.

There remains little research into change of precipitation extremes over the large parts of Himalayan range and little from higher altitudes. Without such work, the exact sensitivity of the

Himalayan range to precipitation change cannot be described properly. Himalayan range within China is a large part of Himalayan range (Fig. 1B), and belongs to Greater Himalaya of high altitudes (Chen et al., 2012). Besides, the impact of the South Asian Summer Monsoon (SASM) on precipitation indices has not been studied adequately. In the study, we investigate the trends of precipitation extremes in Himalayan range within China based on the daily precipitation from 1978 to 2016. Moreover, we furtherly analyze the relationship between the South Asian Summer Monsoon (SASM) and 12 precipitation indices in the region. The study will contribute to a better understanding for changes of precipitation extremes in Himalayan range.

2. Study area and data

On the north, the Himalayan range within China is bordered by the Qinghai-Tibetan Plateau and on the south it is on the Indo-Gangetic Plain, and on the northwest on the Hindu Kush ranges. A continental collision along the convergent boundary between the Plates of Indo-Australian and the Eurasian causes its formation (Yin, 2006). The Himalayan range within China consist metamorphic rock. The region experiences a wide range of climates from humid subtropical weather to cold and dry desert weather. The various climate of Himalayan range within China was influenced by the South Asian Summer monsoon. According to the ‘observed data are continuous and data precipitation series are as long as possible’ rule, 9 meteorological stations were selected to study the changes of precipitation extremes in the Himalayan range within China. The basic information of selected stations is shown in Table 1. The daily precipitation data of selected stations was downloaded from the web site of <http://data.cma.cn/>.

Table 1: Contents of the selected stations

No.	WMO number	Station name	North latitude(°)	East longitude(°)	Elevation (m)
1	55228	Shiquanhe	80.05	32.3	4279
2	55437	Purang	81.15	30.17	3900
3	55664	Tingri	87.05	28.38	4300
4	55655	Nyalam	85.58	28.11	3810
5	55569	Lhazê	87.36	29.05	4000
6	55680	Gyangzê	89.36	28.55	4040
7	55598	Tsedang	91.46	29.16	3560
8	56312	Nyingchi	94.2	29.4	2992
9	56227	Bome	95.46	29.52	2736

Data quality control comprises of two parts. First, from March, 2011 to June, 2012, the quality control of all national meteorological stations (including 9 stations in the paper) had been done by the National Meteorological Information Center of China Meteorological Administration. Second, the RCLimdex V1 software, served as a simple control for the data quality, identifies on a first run erroneous precipitation data, taking precipitation values below 0mm as an example. Additional execution contains identification of potential outliers. In this paper, those outliers have been manually validated, removed or corrected. RHtest V3 software inspected homogeneity assessment of raw precipitation data after data quality control. RCLimdex V1 software and RHtest V3 are downloaded from <http://etccid.pacificclimate.org>.

The trend changes of extreme precipitation indices (Zhang et al., 2011) were revealed by 12 extreme precipitation indices. In accordance with previous researches (Croitoru et al., 2013; Hundedcha and Bárdossy, 2005), those extreme precipitation indices comprehend three types in Himalayan range within China. Table 2 represents the basic information of those indices and its belonging category. The methods for analyzing indices comprise four parts. First, the RCLimDex

software the extreme precipitation indices except wet days (NW). Once daily precipitation is greater or equal to 1 mm, the number of wet days (NW) is counted once. Second, the trends of extreme precipitation indices are calculated by the MAKESENS software. The trend is considered to be statistically large if it is massive at the 5% level using a method named Mann Kendall test. Mann Kendall test can be used in MAKESENS software (Salmi et al., 2002). The Origin and ArcGIS 10.1 software describe the temporal and spatial varieties of indices trends, respectively. Third, according to the software of Statistic Package for Social Science (SPSS), Pearson's correlation and two-tailed t-test are used to detect and estimate correlation coefficient among indices (Li et al., 2012). Fourth, we analyze the relationship between extreme precipitation indices and the South Asian Summer Monsoon (SASM) by using Pearson's correlation and two-tailed t-test methods on account of the SPSS software.

Table 2: Descriptions of extreme precipitation indices

Category	Indices	Full name	Descriptions
Indices based on fixed thresholds	R10 (days)	Heavy precipitation days	Numbers of days per year when daily precipitation $\geq 10\text{mm}$
	R20 (days)	Very heavy precipitation days	Numbers of days per year when daily precipitation $\geq 20\text{mm}$
	R25 (days)	Extremely heavy precipitation days	Numbers of days per year when daily precipitation $\geq 25\text{mm}$
	CDD (days)	Consecutive dry days	Maximum number of consecutive days when daily precipitation $< 1\text{mm}$
	CWD (days)	Consecutive wet days	Maximum number of consecutive days when daily precipitation $> 1\text{mm}$
	R95 (mm)	Precipitation on very wet days	Annual total precipitation $> 95\text{th}$ percentile
	R99 (mm)	Precipitation on extremely wet days	Annual total precipitation $> 99\text{th}$ percentile
Indices based on station-related thresholds	RX1day (mm)	Highest precipitation amount of max one day	Annual maximum precipitation over 1-day intervals
	RX5day (mm)	Highest precipitation of max five day precipitation amount	Annual maximum precipitation sums over 5-day intervals
Non-threshold indices	SDII (mm)	Simple daily intensity index	Annual total precipitation divided by the number of wet days $\geq 1\text{mm}$
	PRCPTOT (mm)	Annual total wet day precipitation	Annual total precipitation from days with precipitation $\geq 1\text{mm}$
	NW (days)	Wet days	Number of days per year with daily precipitation $\geq 1\text{mm}$

3. Results

3.1 Temporal and spatial changes of trends in precipitation extremes

The regionally averaged trends of precipitation indices are revealed in Table 3 from 1978 to 2016. The trends of precipitation indices at individual station were shown in Table 4. Fig. 2 and Fig. 4 and Fig. 6 show the temporal changes of precipitation extreme indices. Fig. 3 and Fig. 5 and Fig. 7 show the spatial changes of precipitation extreme indices. Table 6 shows the correlation coefficients among precipitation indices. Table 7 and Table 8 show the relationship between South Asia Summer Monsoon (SASM) and precipitation extreme indices.

3.1.1 Varieties of trends in fixed thresholds indices

The average regional series has a slight decrease of -0.12 mm/decade over the Himalayan range within China in heavy precipitation days (R10). But the trend is not statistically significant. The time

series of heavy precipitation days (R10) demonstrate the year 2000 has the highest anomaly of 15.8 mm, while the year 2009 has the lowest anomaly of 7.9 mm (Fig. 2). For individual stations, the trends of heavy precipitation days (R10) in five stations are stationary. The other stations show little change, and any changes are not statistically significant (Table 3 and Fig. 3).

Similarly, very heavy precipitation days (R20) showed a statistically insignificant negative slope of -0.2 mm/decade over Himalayan range within China. The highest anomaly of 4.7 mm was observed in 1998, while the lowest anomaly of 1.6 mm was observed in 2009 (Fig. 2). There is a decadal declining pattern from 1997 to 2007 by using a 4-year running mean. Lhazê and Bome stations have a decreasing trend of 0.71 and -0.42 mm/decade, respectively. But the trends of Lhazê and Bome stations are not statistically significant. In other stations, the trends of very heavy precipitation days (R20) are stationary.

Extremely heavy precipitation days (R25) decreased very slightly by -0.1 mm/decade in Himalayan range within China. The highest anomaly of 2.7 mm was observed in 1985, while the lowest anomaly of 0.4 mm was observed in 1992 (Fig. 2). The trends of extremely heavy precipitation days (R25) in every station are stationary. It indicates that the frequency of extremely heavy precipitation days is changeless.

The average regional series has an obvious increase of 3.17 days/decade over the Himalayan range within China in consecutive dry days (CDD), and this trend is statistically significant. The highest anomaly of 150 days was observed in 1984, while the lowest anomaly of 88 days was observed in 1983 (Fig. 2). 2 out of 9 stations have obviously increased trends, while 6 out of 9 stations have obviously increased trends except Nyingchi station. The slightly positive slope is 0.43 days/decade in Nyingchi station. The positive slope of Lhazê and Bome stations are statistically significant, while other stations are not statistically significant.

Table 3 reveal a stationary trend in consecutive wet days (CWD) over the Himalayan range within China. The highest anomaly of 9.8 days was observed in 1998, while the lowest anomaly of 4.9 days was observed in 2009 (Fig. 2). There is a decadal rising pattern from 1987 to 1997 by using a 4-year running mean. 5 out of 9 stations are stationary. The increasing trends of 0.69 and 0.3 days/decade were detected in Tingri and Nyalam stations, respectively. The trend in Tingri station is statistically significant. Lhazê and Gyangzê stations have insignificantly decreasing trends of -0.3 and -0.5 days/decade, respectively (Fig. 3).

Table 3: Regional trends of extreme precipitation indices

Index	Regional trends	Unit
Fixed thresholds indices		
R10	-0.12	days/decade
R20	-0.20	days/decade
R25	-0.10	days/decade
CDD	3.17	days/decade
CWD	0.00	days/decade
Station-related thresholds indices		
R95P	-5.33	mm/decade
R99P	-1.54	mm/decade
Non-threshold indices		
RX1DAY	-0.57	mm/decade
RX5DAY	-0.49	mm/decade
SDII	0.02	mm/decade
PRCPTOP	-5.76	mm/decade
NW	-0.42	days/decade

Trends of statistically significant at 5% level are drawn in bold.

Table 4: Trends of extreme precipitation indices in each station ($10 a^{-1}$)

Station name	R10	R20	R25	CDD	CWD	R95P	R99P	RX1DAY	RX5DAY	SDII	PRCPTOT	NW
Shiquanhe	0.00	0.00	0.00	-1.82	0.00	0.00	0.00	-1.00	-0.72	-0.05	-0.33	0.33
Purang	0.00	0.00	0.00	8.18	0.00	-0.83	0.00	-0.71	-0.29	0.11	-11.43	-2.50
Nyalam	0.83	0.00	0.00	-5.00	0.30	2.70	0.00	0.40	-1.07	0.30	19.47	-1.43
Tingri	0.00	0.00	0.00	5.24	0.69	-4.24	0.00	0.89	0.13	0.00	7.50	-0.59
Lhazê	-1.43	-0.71	0.00	7.59	-0.31	-15.50	0.00	1.90	0.00	-0.17	-30.55	1.25
Gyangzê	0.00	0.00	0.00	2.50	-0.50	3.08	0.00	-0.07	-0.41	0.22	2.47	-0.91
Tsedang	-0.32	0.00	0.00	4.12	0.00	-2.00	0.00	0.00	-3.20	-0.06	-9.04	2.00
Nyingchi	0.00	0.00	0.00	0.43	0.00	-9.04	-1.46	-3.69	-2.50	-0.03	-15.00	-0.63
Bome	0.50	-0.42	0.00	7.86	0.00	-10.43	0.00	-0.50	0.04	0.09	-0.40	-1.25

Trends of statistically significant at 5% level are drawn in bold.

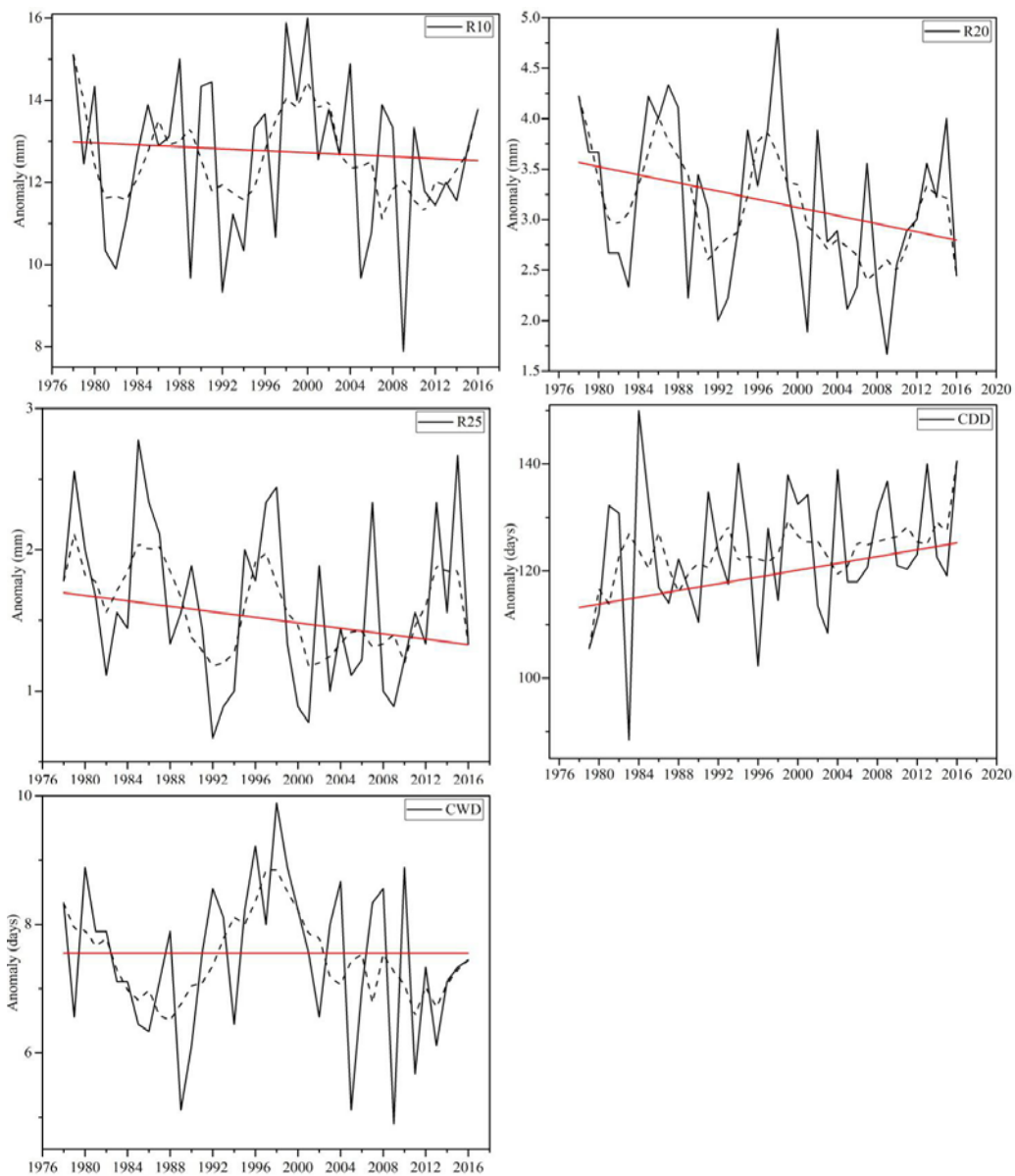


Figure 2: The temporal changes of trends for precipitation extreme indices (R10, R20, R25, CDD and CWD). The black line is the series of indices from 1978 to 2016. The red line is the slope of a linear trend for indices. The dashed black line is the 4-year running mean.

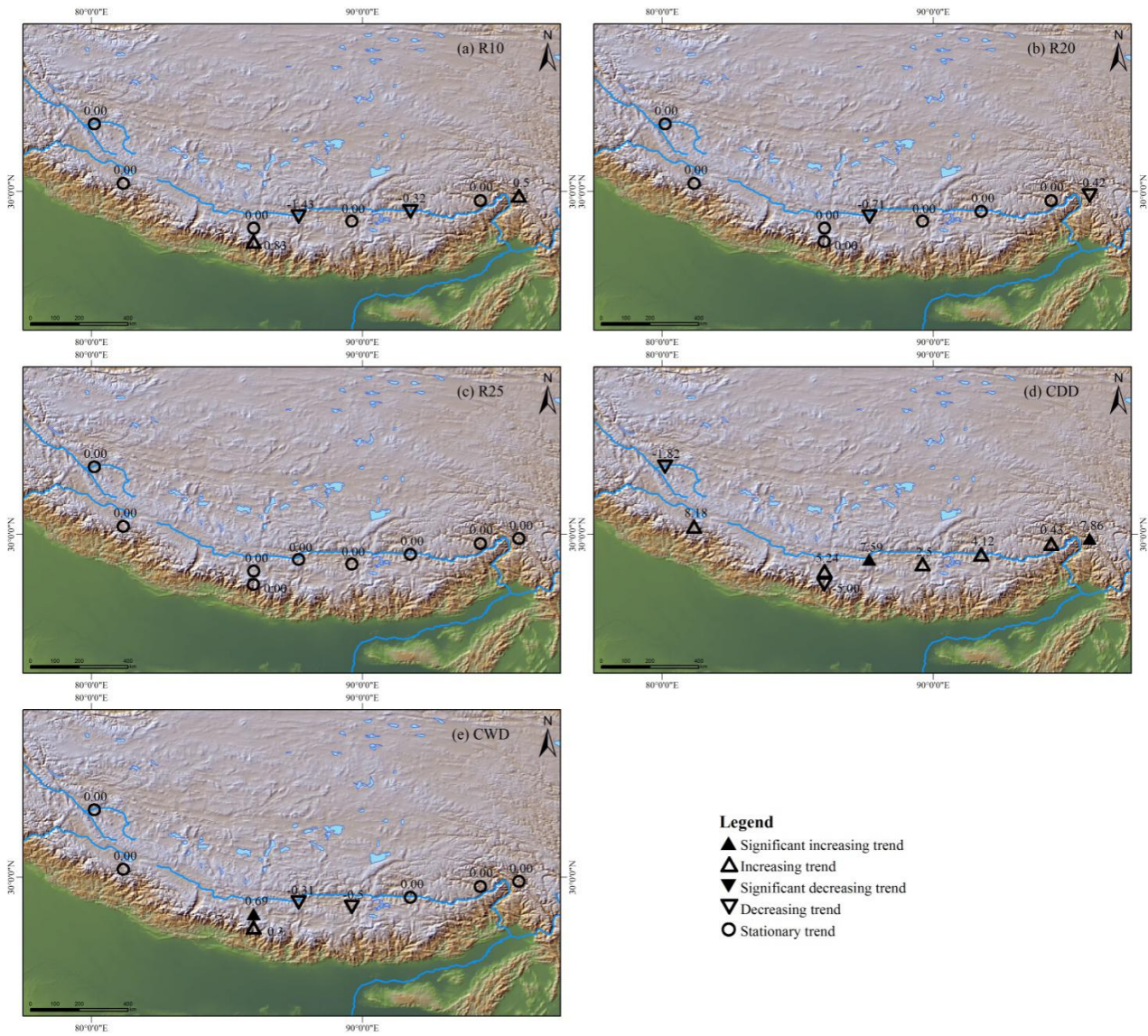


Figure 3: Spatial changes of trends for fixed thresholds indices over Himalayan range within China from 1978 to 2016.

3.1.2 Varieties of trends in station-related thresholds indices

The precipitation on very wet days (R95) showed an obviously decreasing trend of -5.33 mm/decade over Himalayan range within China. This trend is statistically insignificant. The highest anomaly of 140 mm was observed in 1985, while the lowest anomaly of 42 mm was observed in 1992 (Fig. 4). Most of the stations have statistically insignificant decreasing trends except Shiquanhe, Nyalam and Gyangzê stations, which are ranged from -0.83 mm/decade to -15.5 mm/decade. The maximum trend of -15.5 mm/decade was observed in Lhazê station. The Shiquanhe station has a stationary trend. The Nyalam and Gyangzê stations have statistically insignificant increasing trends of 2.70 and 3.08, respectively (Fig. 5).

The very wet days precipitation (R95) showed a decreasing trend of -1.54 mm/decade over Himalayan range within China. The negative slope is statistically insignificant. The highest anomaly of 74 mm was observed in 1985, while the lowest anomaly of 0.2 mm was observed in 1994 (Fig. 4). Most of the stations have stationary trends except Nyingchi station. Nyingchi station has a decreasing

trend of -1.46 mm/decade, but the trend is statistically insignificant (Fig. 5).

3.1.3 Varieties of trends in no-thresholds indices

Max one day precipitation amount (RX1day) showed a statistically insignificant negative slope of -0.57 mm/decade over Himalayan range within China. The highest anomaly of 47 mm/decade was observed in 1988, while the lowest anomaly of 23 mm was observed in 2016 (Fig. 6). There is a decadal rising pattern from 2003 to 2013. Positive and negative slopes are observed in 9 stations, but most of the slopes are statistically insignificant except Nyingchi station (Fig. 7). Nyingchi station has a statistically insignificant decreasing trend of -3.69 mm/decade.

Similarly, max five day precipitation amount (RX5day) showed a statistically insignificant negative slope of -0.49 mm/decade over Himalayan range within China. The highest anomaly of 86 mm/decade was observed in 1988, while the lowest anomaly of 46 mm was observed in 1994 (Fig. 6). The trends of all stations are statistically insignificant. 6 out of 9 stations have decreasing trends with ranging from -0.29 to -3.2 mm/decade (Fig. 7). 2 out of 9 stations have slightly increasing trends of 0.13 and 0.04 mm/decade. The trend of Lhazê station is stationary.

Simple daily intensity index (SDII) showed a slightly increasing trend of 0.2 mm/days/decade over Himalayan range within China. The highest anomaly of 7.1 mm/decade was observed in 1985, while the lowest anomaly of 5.4 mm was observed in 1982 (Fig. 6). Slightly increasing and decreasing trends are observed in 9 stations (Fig. 7). However, the trends are all statistically insignificant.

Annual total wet day precipitation (PRCPTOT) showed an obviously decreasing trend of -5.76 mm/decade over Himalayan range within China. The highest anomaly of 492 mm/decade was observed in 1998, while the lowest anomaly of 273 mm was observed in 2009 (Fig. 6). The trends of all stations are statistically insignificant. 6 out of 9 stations have obviously decreasing trends with ranging from -0.33 to -30.55 mm/decade. 3 out of 9 stations have obviously increasing trends with ranging from 2.47 to 19.47 mm/decade (Fig. 7). The Lhazê station has the largest decreasing trend of -30.55 mm/decade. The Nyalam station has the largest increasing trend of 19.47 mm/decade.

Wet days (NW) showed a slightly decreasing trend of -0.42 days/decade over Himalayan range within China. The highest anomaly of 73 days was observed in 2000, while the lowest anomaly of 44 days was observed in 2009 (Fig. 6). Positive and negative slopes are observed in 9 stations (Fig. 7). But the trends are statistically insignificant except Purang station. Purang station has a statistically significant decreasing trend of -2.5 days/decade.

3.2 Varieties of trends in monthly precipitation extremes

The trends of nine months in RX1day are negative except January, February and December (Table 5). The trends are not statistically significant except December. The December of RX1day has a statistically significant decreasing trend of -0.68 mm/decade. Besides, 3 out of 12 months have slightly increasing trend from 0.05 to 0.78 mm/decade. While other months showed decreasing trend from 0.13 to 0.78. For RX5day, slightly increasing and decreasing trends are observed from January to December. The February has the largest increasing trends of 0.91 mm/decade. The July has the largest decreasing trends of 1.85 mm/decade. The trends are not statistically significant except December. The December of RX5day has a statistically significant decreasing trend of -0.98 mm/decade.

Table 5: Trends in precipitation extremes indices from January to December ($10 a^{-1}$)

Name	Jan	Feb	Mar	Apr	May	Jun	Jul	Aug	Sep	Oct	Nov	Dec
RX1DAY	0.26	0.78	-0.54	-0.13	0.05	-0.41	-0.40	-0.13	-0.78	-0.13	-0.19	-0.68
RX5DAY	-0.25	0.91	-0.57	0.25	0.56	-0.81	-1.85	0.32	-1.15	-1.21	-0.11	-0.98

Trends of statistically significant at 5% level are drawn in bold.

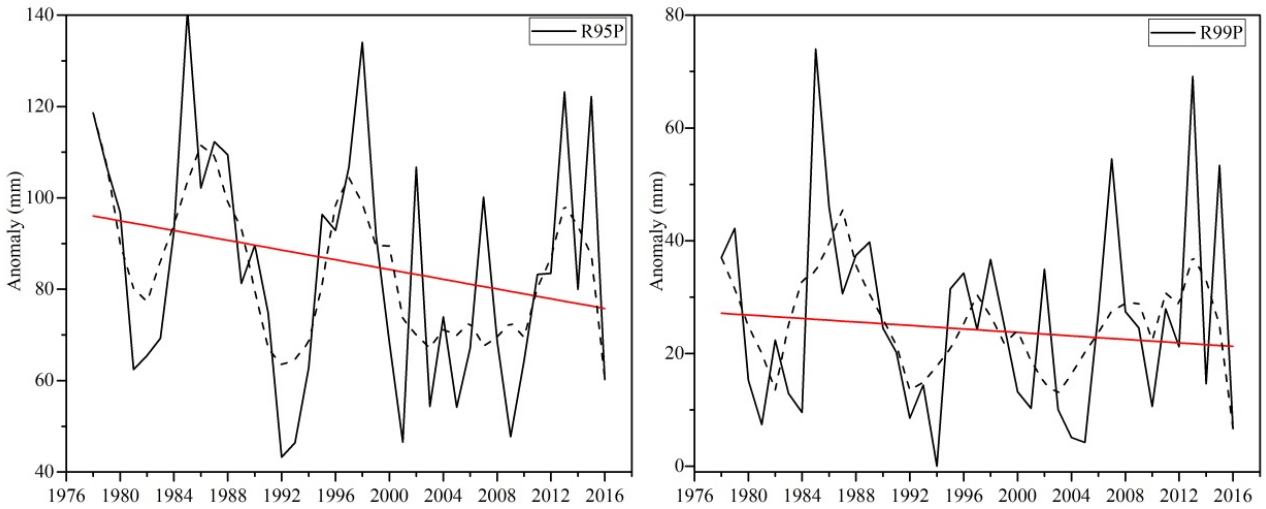


Figure 4: The temporal changes of trends for precipitation extreme indices (R95 and R99). The black line is the series of indices. The red line is the slope of a linear trend for indices. The dashed black line is the 4-year running mean.

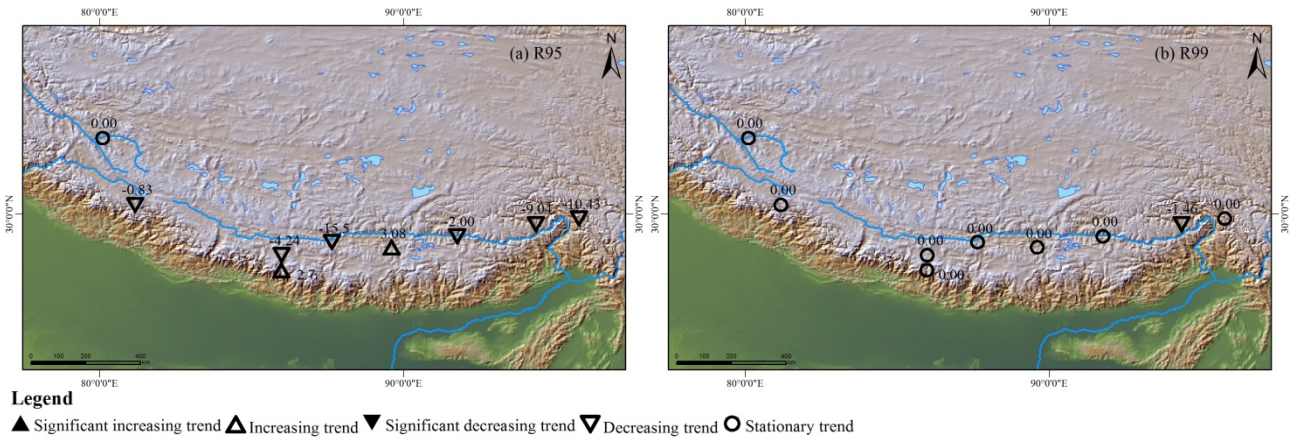


Figure 5: Spatial changes of trends for station-related thresholds indices over Himalayan range within China from 1978 to 2016.

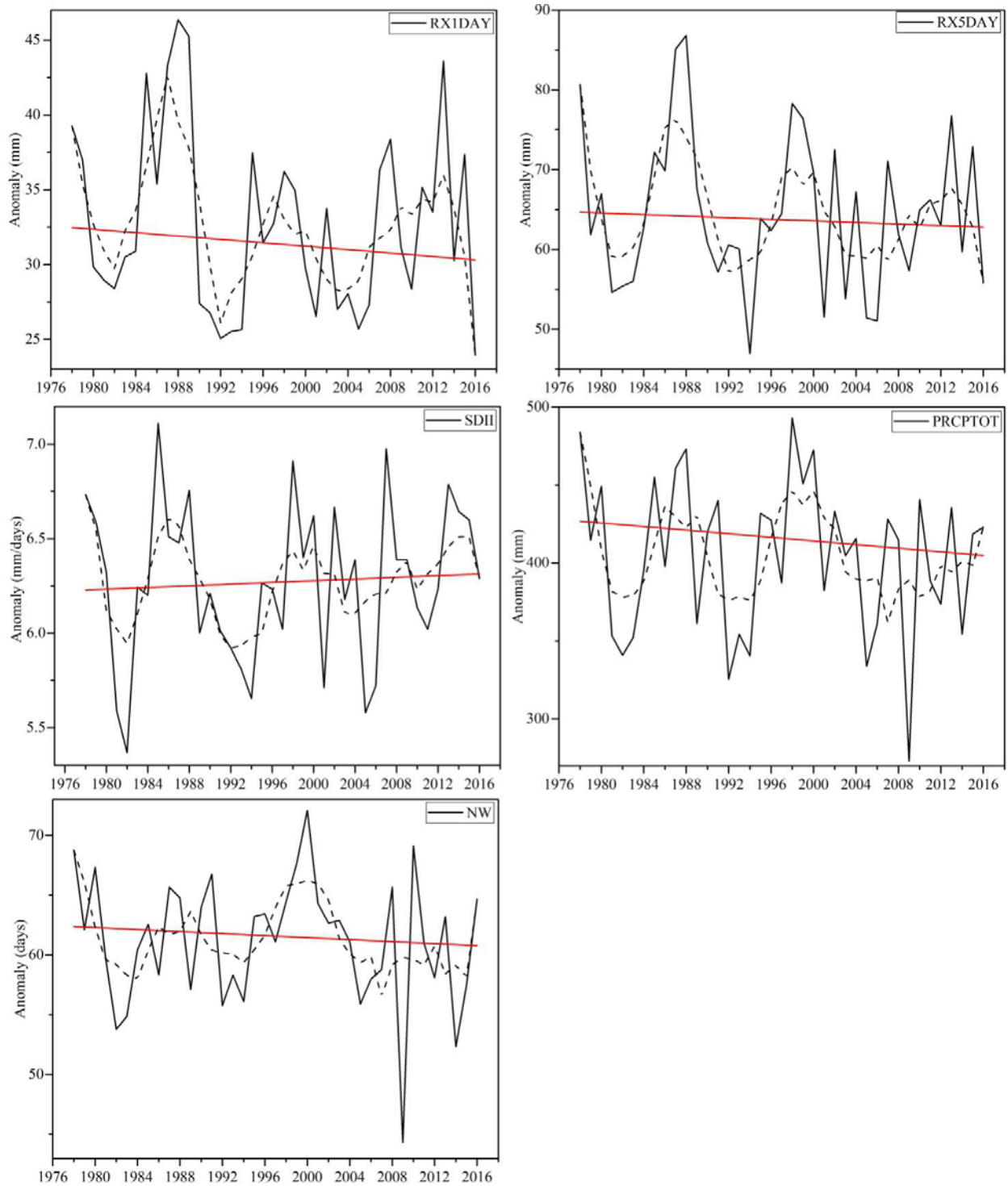


Figure 6: The temporal changes of trends for precipitation extreme indices (RX1day, RX5day, SDII, PRCPTOT and NW). The black line is the series of indices. The red line is the slope of a linear trend for indices. The dashed black line is the 4-year running mean.

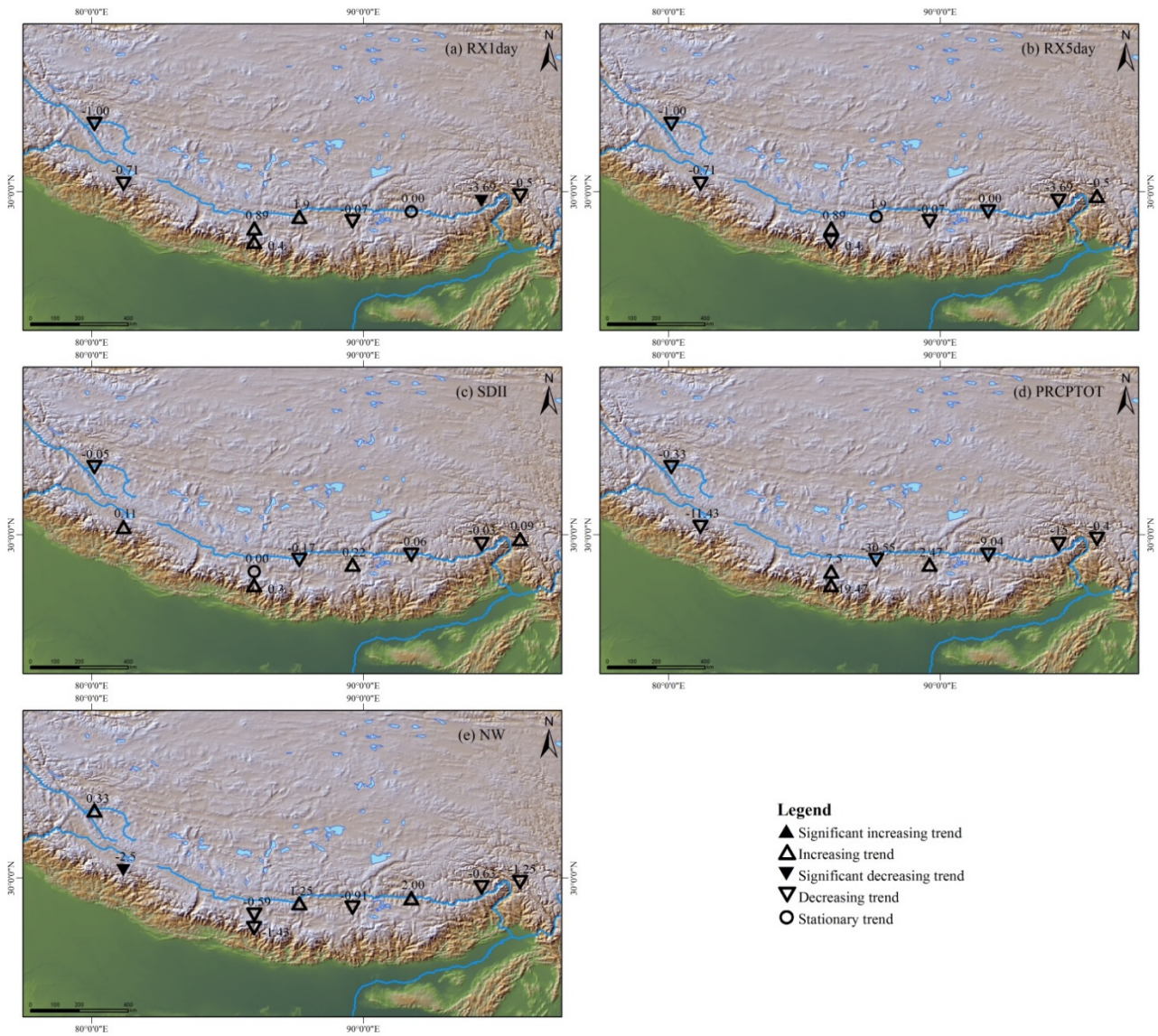


Figure 7: Spatial changes of trends for no-thresholds indices over Himalayan range within China from 1978 to 2016.

3.3 Correlations among extreme precipitation indices

The consecutive dry day (CDD) scarcely correlates with other indices (Table 6). Besides, the correlations between the consecutive wet day (CWD) and other indices are also weak. However, the connections between most of the indices are tight except CDD and CWD. Therefore, we analysed the correlations between PRCPTOT, SDII and 9 extreme precipitation indices (Table 6). The 9 extreme precipitation indices contains the indices according to fixed thresholds (R10, R20, R25), indices based on station-related thresholds (R95 and R99), and non-threshold indices (RX1day, RX5day, PRCPTOT, NW). The average connections between total precipitation and R10, R20 and R25 are tighter ($r > 0.75$) than with SDII. The great connection ($r=0.73$) between SDII and R95 are tighter than with total precipitation ($r=0.62$). Besides, the significant correlation ($r=0.66$) between SDII and R99 are also stronger than with total precipitation ($r=0.35$). The tight connections between total precipitation with RX1day and RX1day ranged from 0.39 to 0.67 are weaker than with SDII ranged from 0.62 to 0.74. The significant correlation ($r=0.97$) between total precipitation and PRCPTOT is strongest. The

significant correlation between total precipitation and PRCPTOT is 0.65. The significant correlation (r=0.87) between total precipitation and NW is equal with SDII.

Table 6: Correlation coefficients between extreme precipitation indices and total precipitation.

	Total precipitation	R10	R20	R25	CDD	CWD	R95P	R99P	RX1DAY	RX5DAY	SDII	PRCPTOT	NW
Total precipitation	1												
R10	0.93**	1											
R20	0.68**	0.61**	1										
R25	0.44**	0.33*	0.80**	1									
CDD	-0.18	-0.15	-0.24	-0.23	1								
CWD	0.52**	0.53**	0.23	-0.03	-0.10	1							
R95P	0.62**	0.51**	0.92**	0.88**	-0.23	0.07	1						
R99P	0.35*	0.22	0.58**	0.74**	-0.16	-0.17	0.78**	1					
RX1DAY	0.39**	0.23	0.58**	0.57**	-0.17	-0.13	0.75**	0.79**	1				
RX5DAY	0.67**	0.56**	0.73**	0.52**	-0.21	0.21	0.77**	0.61**	0.78**	1			
SDII	0.66**	0.61**	0.66**	0.60**	-0.17	0.13	0.73**	0.66**	0.62**	0.74**	1		
PRCPTOT	0.97**	0.93**	0.73**	0.47**	-0.20	0.48**	0.68**	0.41**	0.46**	0.72**	0.65**	1	
NW	0.87**	0.81**	0.40**	0.15	-0.11	0.51**	0.32*	0.07	0.18	0.44**	0.29*	0.87**	1

‘**’ symbol means the statistically significant at the 1% level, ‘*’ symbol means the statistically significant at the 5% level.

3.4 Relationship between the extreme precipitation indices and the South Asian Summer Monsoon

The description of monsoon active/break period is represented as follows. The year is a strong monsoon year when the monsoon index of this year is greater than or equal to one standard deviation 1.4 m/s, in comparison to the weak monsoon year when the monsoon index of this year is less than 1.4 m/s (Zhang et al., 2015; Zhou et al., 2013). Based this definition, we calculated the regionally averaged values of extreme precipitation indices during the active and break period (Table 7). The data of the monsoon index of the South Asia Summer Monsoon (SASM) from 1978 to 2016 is downloaded from the website of <http://ljp.lasg.ac.cn>.

The trend changes of most precipitation extreme indices in the Himalayan range within China were impacted by the South Asia Summer Monsoon evolution. The values of consecutive dry days (CDD) during break period are less than that during active period over the Himalayan range within China. The values of extremely heavy precipitation days (R25) are increasing during the monsoon active period, except June. The values of extremely wet day precipitation (R99P) and simple daily intensity index (SDII) are increasing during the monsoon active period, except June and July. Wet day precipitation (PRCPTOT) and very heavy precipitation days (R20 mm) and precipitation on very wet days (R95P) and maximum 1-day precipitation (RX1day) and maximum 5-day precipitation (RX5day) are strengthened in July and September during the monsoon active period. Comparatively, the heavy precipitation days (R10 mm) are strengthening only in September during the monsoon active period. However, the consecutive wet days (CWD) and wet days (NW) are smaller during the monsoon active period from June to September. In the averaged monsoon period (JJAS), the values of CDD, R25, R95P, R99P, RX1DAY, RX5DAY and SDII are increasing during the monsoon active period, while the values of the other precipitation extreme indices are wakening during the monsoon active period. From the above, the values of consecutive dry days (CDD) are increasing in the monsoon active period of June, July, August, September and JJAS, this result shows that the consecutive dry days

(CDD) is more sensitive to the South Asia summer monsoon (SASM) than that of the other precipitation extreme indices.

We also analysis the relationship based on the correlation coefficient between the precipitation extreme indices and SASM (Table 8). There are coherently positive correlations between consecutive dry day (CDD) and the SASM from June to September. Additionally, the positive correlations between the other precipitation indices and the SASM mainly exist in August, while negative correlations of that are exist in June and July and September. Obviously, the correlation coefficients of all precipitation extreme indices and the SASM are not statistically significant (Table 8). The correlations between most of precipitation indices and the SASM are slightly negative in the averaged monsoon period (JJAS), except R25 and SDII. Statistically significant correlations are found in CWD, R10, NW with the SASM.

Table 7: The summed values of the extreme precipitation indices in the monsoon active period (AP) and the monsoon break period (BP)

	June		July		August		September		JJAS	
	AP	BP	AP	BP	AP	BP	AP	BP	AP	BP
R10	11.33	12.98	12.36	12.59	11.67	12.66	13.00	12.52	12.13	12.65
R20	2.81	3.25	3.31	3.11	3.00	3.16	3.56	3.10	3.13	3.14
R25	1.42	1.67	1.73	1.58	1.64	1.60	2.11	1.56	1.76	1.57
CDD	127.74	120.09	126.82	121.35	128.31	121.34	125.37	121.78	122.78	121.90
CWD	7.21	7.53	6.80	7.54	6.72	7.53	7.33	7.46	7.05	7.53
R95P	75.42	87.83	88.16	84.14	81.16	85.05	99.90	83.38	84.80	84.62
R99P	18.93	28.26	23.72	26.19	28.19	25.61	35.42	25.08	26.10	25.82
RX1DAY	30.38	33.56	33.08	32.69	31.38	32.90	34.72	32.58	33.04	32.68
RX5DAY	59.64	66.25	65.39	64.44	61.79	64.88	65.24	64.50	65.38	64.38
SDII	6.20	6.30	6.21	6.28	6.41	6.26	6.59	6.25	6.45	6.24
PRCPTOT	370.47	415.65	406.19	403.75	371.42	407.79	412.47	403.36	397.74	405.45
NW	58.10	62.31	60.98	61.27	55.22	61.92	60.44	61.30	59.38	61.64

The monsoon indexes of JJAS are an average of all monsoon indexes from June to September.

Table 8: Correlation coefficients between the South Asian Summer Monsoon (SASM) and the extreme precipitation indices from June to September.

	Jun	July	August	September	JJAS
CDD	0.13	0.06	0.03	0.19	-0.01
CWD	-0.11	-0.22	-0.11	-0.18	-0.33*
PRCPTOT	-0.26	-0.18	-0.03	-0.10	-0.26
R10	-0.19	-0.29	-0.06	-0.10	-0.32*
R20	-0.10	-0.04	0.11	-0.06	-0.11
R25	-0.05	-0.04	0.14	0.15	0.03
R95P	-0.09	-0.04	0.15	-0.03	-0.08
R99P	-0.18	-0.19	0.15	-0.04	-0.02
RX1DAY	-0.20	-0.09	0.09	-0.09	-0.01
RX5DAY	-0.22	-0.06	0.14	-0.14	-0.04
SDII	0.03	-0.25	0.22	-0.13	0.02
NW	-0.27	-0.13	-0.24	-0.07	-0.36*

‘*’ symbol means the statistically significant at the 5% level. The monsoon indexes of JJAS are the average of all monsoon indexes from June to September.

4. Conclusions

For analyzing the temporal and spatial changes of precipitation extreme, we know only the consecutive dry days (CDD) has a statistically significant increasing trend of 3.17 days/decade over Himalayan range within China. Most of the other indices have decreasing trends for regional pattern except CWD and SDII. For individual stations, many stationary trends are observed in heavy, very heavy and extremely heavy precipitation days (R10, R20 and R25), especially, the trends of number of extremely heavy precipitation days (R25) are all stationary, indicating that the annual occurrence of extremely heavy precipitation is solid from 1978 to 2016, the huge natural disasters maybe not triggered by the extremely heavy precipitation, such as Yigong landslide occurred on April 9th, 2000 and Cirenmacuo GLOF occurred on July, 1981. Most of the stations show the increasing trends in consecutive dry days (CDD). The positive slope of Lhazê and Bome stations are statistically significant in CDD. 5 out of 9 stations have stationary trends in consecutive wet days (CWD). We detect that the consecutive wet days (CWD) of Tingri station has a statistically significant increasing trend. Most of the precipitations on very wet days (R95) have decreasing trends, but they are not statistically significant. Most of the precipitations on extremely wet days (R99) have stationary trends. Increasing and decreasing trends are observed in RX1day, RX5day, SDII and NW. The trends of individual station are very large in PRCPTOT. The Lhazê station has the largest decreasing trend of -30.55 mm/decade in PRCPTOT, and the Nyalam station has the largest increasing trend of 19.47 mm/decade in PRCPTOT. The changes of are obvious differences in monthly RX1day and RX5day. Finally, we can conclude that the temporal and spatial changes of precipitation extreme indices are irregular in Himalayan range with China, and this result is identical to the other research results (El Kenawy et al., 2011; Vincent et al., 2011; Zhang et al., 2017).

There are 4950 glacial lakes in 2015 cover a total area of 455.3 ± 72.7 km² in Himalayan range, and Himalayan glacial lakes expanded by approximately 14.1% from 1990 to 2015 (Nie et al., 2017). Under global warming, the rapidly expanding glacial lakes may have potential outburst risk (Aggarwal et al., 2017; Nagai et al., 2017; Rounce et al., 2017). Precipitation is a major water supply for glacial lakes. From our research results, there were significant correlations between annual total precipitation and precipitation extremes indices, except consecutive dry days (CDD). Therefore, extreme precipitation indices have good indicative functions for outburst risk of glacial lakes in Himalayan range with China.

Acknowledgements

The study was supported by Sichuan Science and Technology Program (Grant Nos. 2021YFG0259), and supported by the opening project of Sichuan Province University Key Laboratory of Bridge Non-destruction Detecting and Engineering Computing (Grant Nos. 2020QZJ02), and supported by the talent introduction project of Sichuan University of Science & Engineering (Grant Nos. 2018RCL09).

References

- [1] Aggarwal, S., Rai, S.C., Thakur, P.K., Emmer, A., 2017. Inventory and recently increasing GLOF susceptibility of glacial lakes in Sikkim, Eastern Himalaya. *Geomorphology* 295, 39-54.
- [2] Baidya, S.K., Shrestha, M.L., Sheikh, M.M., 2008. Trends in daily climatic extremes of temperature and precipitation in Nepal. *J Hydrol Meteorol* 5, 38-51.
- [3] Chen, N., Hu, G., Deng, W., Khanal, N.R., Zhu, Y., Han, D., 2012. Water Hazards in the Trans-boundary Kosi River Basin. *Natural Hazards & Earth System Sciences* 13, 795-808.
- [4] Chen, X., Cui, P., Li, Y., Yang, Z., Qi, Y., 2007. Changes in glacial lakes and glaciers of post-1986 in the Poiqu River basin, Nyalam, Xizang (Tibet). *Geomorphology* 88, 298-311.

- [5] Croitoru, A.E., Chitoroiu, B.C., Todorova, V.I., Torică, V., 2013. Changes in precipitation extremes on the Black Sea Western Coast. *Global & Planetary Change* 102, 10-19.
- [6] Delaney, K.B., Evans, S.G., 2015. The 2000 Yigong landslide (Tibetan Plateau), rockslide-dammed lake and outburst flood: Review, remote sensing analysis, and process modelling. *Geomorphology* 246, 377-393.
- [7] Ding, L., Spicer, R.A., Yang, J., Xu, Q., Cai, F., Li, S., Lai, Q., Wang, H., Spicer, T.E.V., Yue, Y., Shukla, A., Srivastava, G., Khan, M.A., Bera, S., Mehrotra, R., 2017. Quantifying the rise of the Himalaya orogen and implications for the South Asian monsoon. *Geology* 45, 215-218.
- [8] El Kenawy, A., López-Moreno, J.I., Vicente-Serrano, S.M., 2011. Recent trends in daily temperature extremes over northeastern Spain (1960–2006). *Natural Hazards and Earth System Science* 11, 2583-2603.
- [9] Hundedcha, Y., Bárdossy, A., 2005. Trends in daily precipitation and temperature extremes across western Germany in the second half of the 20th century. *International Journal of Climatology* 25, 1189–1202.
- [10] Li, Z., He, Y., Wang, C., Wang, X., Xin, H., Zhang, W., Cao, W., 2011. Spatial and temporal trends of temperature and precipitation during 1960–2008 at the Hengduan Mountains, China. *Quaternary International* 236, 127-142.
- [11] Li, Z., He, Y., Wang, P., Theakstone, W.H., An, W., Wang, X., Lu, A., Zhang, W., Cao, W., 2012. Changes of daily climate extremes in southwestern China during 1961–2008. *Global & Planetary Change* 80–81, 255-272.
- [12] Lu, H., Du, J., Yuan, L., Liao, J., 2014. Variation characteristic of extreme precipitation events over Mt. Qomolangma region in China from 1971 to 2012. *Journal of Glaciology and Geocryology* 36, 563-572.
- [13] Nagai, H., Ukita, J., Narama, C., Fujita, K., Sakai, A., Tadono, T., Yamanokuchi, T., Tomiyama, N., 2017. Evaluating the Scale and Potential of GLOF in the Bhutan Himalayas Using a Satellite-Based Integral Glacier–Glacial Lake Inventory. *Geosciences* 7, 77.
- [14] Nie, Y., Sheng, Y., Liu, Q., Liu, L., Liu, S., Zhang, Y., Song, C., 2017. A regional-scale assessment of Himalayan glacial lake changes using satellite observations from 1990 to 2015. *Remote Sensing of Environment* 189, 1-13.
- [15] Ning, B., Yang, X., Chang, L., 2012. Changes of temperature and precipitation extremes in Hengduan Mountains, Qinghai-Tibet Plateau in 1961–2008. *Chinese Geographical Science* 22, 422-436.
- [16] Rounce, D., Watson, C.S., McKinney, D., 2017. Identification of Hazard and Risk for Glacial Lakes in the Nepal Himalaya Using Satellite Imagery from 2000–2015. *Remote Sensing* 9, 654.
- [17] Salmi, T., Määttä, A., Anttila, P., Ruoho-Airola, T., Amnell, T., 2002. Detecting Trends of Annual Values of Atmospheric Pollutants by the Mann-Kendall Test and Sen's Solpe Estimates the Excel Template Application MAKESENS. *Universitas Gadjah Mada* 31, 1-35.
- [18] Shang, Y., Yang, Z., Li, L., Liu, D.A., Liao, Q., Wang, Y., 2003. A super-large landslide in Tibet in 2000: background, occurrence, disaster, and origin. *Geomorphology* 54, 225-243.
- [19] Sigdel, M., Ma, Y., 2016. Variability and trends in daily precipitation extremes on the northern and southern slopes of the central Himalaya. *Theoretical and Applied Climatology* 130, 571-581.
- [20] Tian, L., Yao, T., Gao, Y., Thompson, L., Mosley-Thompson, E., Muhammad, S., Zong, J., Wang, C., Jin, S., Li, Z., 2016. Two glaciers collapse in western Tibet. *Journal of Glaciology* 63, 194-197.
- [21] Vincent, L.A., Aguilar, E., Saindou, M., Hassane, A.F., Jumaux, G., Roy, D., Booneedy, P., Virasami, R., Randriamarolaza, L.Y.A., Faniriantsoa, F.R., Amelie, V., Seeward, H., Montfraix, B., 2011. Observed trends in indices of daily and extreme temperature and precipitation for the countries of the western Indian Ocean, 1961–2008. *Journal of Geophysical Research* 116, D10108.
- [22] Wang, S., Zhang, M., Wang, B., Sun, M., Li, X., 2013. Recent changes in daily extremes of temperature and precipitation over the western Tibetan Plateau, 1973–2011. *Quaternary International* 313-314, 110-117.
- [23] Wang, W., Gao, Y., Anaconda, P.I., Lei, Y., Xiang, Y., Zhang, G., Li, S., Lu, A., 2015. Integrated hazard assessment of Cirenmaco glacial lake in Zhangzangbo valley, Central Himalayas. *Geomorphology*.
- [24] Yin, A., 2006. Cenozoic tectonic evolution of the Himalayan orogen as constrained by along-strike variation of structural geometry, exhumation history, and foreland sedimentation. *Earth-Science Reviews* 76, 1-131.
- [25] Zhang, J.-Y., Yin, A., Liu, W.-C., Ding, L., Xu, X.-M., 2016. First geomorphological and sedimentological evidence for the combined tectonic and climate control on Quaternary Yarlung river diversion in the eastern Himalaya. *Lithosphere* 8, 293-316.
- [26] Zhang, J., Shen, X., Wang, B., 2015. Changes in precipitation extremes in Southeastern Tibet, China. *Quaternary International* 380-381, 49-59.
- [27] Zhang, K., Pan, S., Cao, L., Wang, Y., Zhao, Y., Zhang, W., 2014. Spatial distribution and temporal trends in precipitation extremes over the Hengduan Mountains region, China, from 1961 to 2012. *Quaternary International* 349, 346-356.
- [28] Zhang, M., Chen, Y., Shen, Y., Li, Y., 2017. Changes of precipitation extremes in arid Central Asia. *Quaternary International* 436, 16-27.
- [29] Zhang, X., Alexander, L., Hegerl, G.C., Jones, P., Tank, A.K., Peterson, T.C., Trewin, B., Zwiers, F.W., 2011. Indices for monitoring changes in extremes based on daily temperature and precipitation data. *Wiley Interdisciplinary Reviews Climate Change* 2, 851–870.

- [30] Zhou, J.W., Cui, P., Hao, M.H., 2016. *Comprehensive analyses of the initiation and entrainment processes of the 2000 Yigong catastrophic landslide in Tibet, China. Landslides 13, 39-54.*
- [31] Zhou, L., Zhu, J., Zou, H., Ma, S., Li, P., Zhang, Y., Huo, C., 2013. *Atmospheric moisture distribution and transport over the Tibetan Plateau and the impacts of the South Asian summer monsoon. Acta Meteor. Sinica 27, 819-831.*